ELSEVIER

International Journal of Mass Spectrometry 182/183 (1999) 149–161

International Journal of Mass Spectrometry

Bond strengths in cyclopentadienyl metal carbonyl anions

Lee S. Sunderlin[a,*], Robert R. Squires[b,1]

[a] *Department of Chemistry, Northern Illinois University, DeKalb, IL 60115, USA*
[b] *Department of Chemistry, Purdue University, West Lafayette, IN 47907, USA*

Received 16 July 1998; accepted 10 September 1998

Abstract

Energy-resolved collision-induced dissociation of metal cyclopentadienyl carbonyl anions $CpM(CO)_x^-$ (Cp=*c*-C_5H_5, M=V, Cr, Mn, Fe, Co) is used to determine metal–carbonyl bond energies in these systems. These bond energies are, in general, slightly stronger than those for the corresponding homoleptic metal carbonyl anions. The bond strength in $CpCo(CO)_2^-$, a 19-electron complex, is notably weaker than most of the others. D[$CpMn^-$-CO] is also weak; this is attributed to a mismatch in the electronic ground states of $CpMn^-$ and $CpMnCO^-$. D[$CpCo^-$-CO], on the other hand, is substantially larger than the others, and is comparable to the bond energy measured in solution for $CpMn(CO)_3$. (Int J Mass Spectrom 182/183 (1999) 149–161) © 1999 Elsevier Science B.V.

Keywords: Flowing afterglow; Collision-induced dissociation (CID); Bond energies; Cyclopentadienyl metal carbonyls

1. Introduction

The metal carbonyls $M(CO)_x$ and metallocenes Cp_2M (Cp=η^5-C_5H_5) are prototypical organometallic compounds, as well as models for metal–ligand bonding. Much of the earliest organometallic thermochemistry is devoted to these species, and the average metal–ligand bond strengths for coordinatively saturated transition metal carbonyl and cyclopentadienyl complexes derived from calorimetric measurements have been a major influence on the understanding of metal–ligand bonding trends. Numerous accounts of the periodic trends in these properties have appeared [1–4]. However, the thermochemistry of the more complex mixed species $CpM(CO)_x$ is not as well studied. As long ago as 1960, it was noted that the cyclopentadienyl group often deactivates CO ligands towards substitution [5]. More recently, two groups used photoacoustic calorimetry to measure the first M–CO bond strength in $CpMn(CO)_3$, both obtaining the value of 230 kJ mol^{-1} [6,7]. This bond is impressively strong in comparison to the bond strengths in the 18-electron metal carbonyls: D[$(CO)_5Cr$-CO] = 154 ± 8 kJ mol^{-1} [8], D[$(CO)_4Fe$-CO] = 174 ± 8 kJ mol^{-1} [8], and D[$(CO)_3Ni$-CO] = 90 ± 2 kJ mol^{-1} [9].

We have recently measured M–CO bond energies for an extensive series of first-row metal carbonyl anions, $M(CO)_x^-$, using energy-resolved collision-induced dissociation (CID) [10,11]. Analogous measurements have also been made for the metal carbonyl cations, $M(CO)_x^+$ [12,13]. The majority of the anion bond energies are in the range of 150–185 kJ mol^{-1},

* Corresponding author.

[1]Deceased September 30, 1998.

Dedicated to the memory of our friend and colleague Ben Freiser.

PII S1387-3806(98)14230-6

and none were measured to be higher. The M–CO bond strengths in metal carbonyl anions are generally greater than in the corresponding neutral and cationic species; this can be understood in terms of increased π back-bonding in the anions. This fact, along with the high M–CO bond energy measured for $CpMn(CO)_3$, suggests that certain cyclopentadienyl metal carbonyl anions, $CpM(CO)_x^-$, might have the strongest M–CO bond strengths of all. Therefore, we have performed energy-resolved CID experiments with these ions to measure the metal–ligand bond strengths and determine the effects of the Cp ligand on metal–carbonyl bond strengths.

The cyclopentadienyl metal carbonyls have been previously examined using mass spectrometry. Winters and Kiser reported the positive and negative ion mass spectra of the cobalt, manganese, and vanadium cyclopentadienyl carbonyls, and determined some approximate metal–CO bond energies for the cationic species by measuring the difference in the appearance potentials of $CpM(CO)_x^+$ fragments [14]. Gregor and co-workers [15] reported additional fragment ions in the electron impact mass spectra of the neutrals studied by Winters and Kiser. Other groups have measured appearance potentials for ions derived from $CpMn(CO)_3$ and related compounds [16,17]. Corderman and Beauchamp [18] and McDonald and Schell [19] have described the gas-phase ligand substitution reactions of $CpCo(CO)_x^-$ ($x = 1,2$), and Nibbering and co-workers have studied the reactions of various anions with $CpCo(CO)_2$ [20]. General reviews of the ion–molecule reactions of organometallic anions have been published [21,22].

2. Experimental

All experiments were performed with a flowing afterglow triple quadrupole apparatus described previously [23,24]. The operating conditions in the 7.3 cm inner diameter (i.d.) $\times$ 100 cm flow tube were P = 0.40 Torr, flow (He) = 190 STP $cm^3\ s^{-1}$ and T = 298 K. The precursor neutrals $CpV(CO)_4$, $[CpCr(CO)_3]_2$, $CpMn(CO)_3$, $[CpFe(CO)_2]_2$ or $CpFe(CO)_2I$, $CpCo(CO)_2$, and $[CpNiCO]_2$ were added to the upstream end of the flow tube. Ionization was caused by either an electron impact (EI) source operating at 70 V and $\sim$ 0.5 mA emission, or a dc discharge source operating at $\sim$ 800 V and 3 mA emission [10]. Pure He buffer gas is used with the EI source and a 10:1 He:Ar mixture with the dc discharge source. Ions are thermalized by about 10^5 collisions with the bath gas. For the neutral precursors used in the present study, it was possible to form sufficient amounts of eight different $CpM(CO)_x^-$ anions to measure thresholds for loss of a carbonyl ligand.

Ions in the flow tube are gently extracted through a 1 mm orifice into a region of differential pumping and then focused into the Extrel triple quadrupole mass analyzer. The desired reactant ion is selected with the first quadrupole and injected into the rf-only, gas-tight central quadrupole (Q2) with an axial kinetic energy determined by the Q2-rod offset voltage. Argon is maintained in Q2 at a pressure of $\leq$ 0.04 mTorr. Use of Ar as the CID target gas for metal carbonyl anions has been tested previously [10]. Fragment ions resulting from single or multiple ligand loss upon collision with Ar are efficiently contained in Q2 and extracted by a low voltage exit lens into the third quadrupole, which is maintained at a constant attractive voltage (3–7 V), with respect to the variable Q2 rod voltage. Ion detection is carried out with a conversion dynode and an electron multiplier operating in pulse-counting mode.

Detailed accounts of the data collection procedures and analysis method for CID threshold energy measurements have been provided [10,11]. Briefly, the axial kinetic energy of the mass-selected reactant ion is scanned while monitoring the intensity of the CID fragment ion formed in Q2 under single-collision conditions. The center-of-mass collision energy E_{CM} for the system is given by $E_{CM} = E_{lab}[m/(M + m)]$, where E_{lab} is the nominal lab energy and M and m represent the masses of the reactant ion and neutral target, respectively. The energy axis origin is verified by retarding potential analysis, and the reactant ion kinetic energy distribution is found to have a near-Gaussian shape with a full width at half maximum (FWHM) of 0.5–2 eV (lab). An uncertainty of $\pm$ 0.15

eV in the lab frame energy scale is included in the uncertainty of the derived thresholds. Absolute cross sections (σ_p) are calculated by use of $\sigma_p = I_p/INl$, where I_p and I are the measured intensities for the product and reactant ion beams, respectively, N is the number density of the neutral target, and l is the effective path length for reaction (24 ± 4 cm) [24].

Collision of the ion with more than one rare gas atom can lead to multiple energy deposition interactions and dissociation below the threshold energy. Ideally, data obtained at several different target gas pressures is extrapolated to zero pressure to derive cross sections under single-collision conditions. In the case of the present data, instability of the reactant ion beam renders this procedure impractical. Instead, the neutral target gas pressure in Q2 is kept low enough (≤ 0.04 mTorr) to ensure predominantly single collision conditions. Under these conditions, less than ~ 3% of the ions that collide with the target gas have another collision. Comparison of thresholds from data sets collected at different pressures indicates that for the pressure range used, the effect of multiple collisions is negligible.

Phase incoherence between the quadrupoles of the triple quadrupole mass analyzer causes oscillations in the apparent intensity of the reactant ion, but not the CID product ions, as the Q2 offset voltage is scanned [25]. For this reason, the intensity of the reactant ion beam is estimated to be equal to the maximum transmitted intensity in the region of the threshold for dissociation. The absolute cross sections may also be in error because of different collection or detection efficiencies for the reactant and product ions. These two factors lead to inaccuracies in the absolute cross sections, which have an estimated uncertainty of a factor of two. Relative cross sections are more reliable (~ ± 50%).

Most reagents were obtained from commercial sources and used as received. $CpV(CO)_4$ and $[CpFe(CO)_2]_2$ were obtained from Alfa; $Cr(CO)_6$, $CpFe(CO)_2I$, $CpCo_2(CO)_2$, and $[CpNiCO]_2$ were obtained from Aldrich; and $CpMn(CO)_3$ was obtained from Thiokol. $[CpCr(CO)_3]_2$ was synthesized as described previously [26].

2.1. CID threshold measurement and analysis

The activation energy for reactant ion dissociation is derived from the product ion appearance curve by means of a fitting procedure based on the model function given by Eq. (1), [10,24,27] where $\sigma(E)$ is the cross section for formation of the product ion

$$\sigma(E) = \sigma_o \sum_i [\, g_i P_D(E,E_i,\tau)(E + E_i - E_\tau)^n/E] \quad (1)$$

at center-of-mass collision energy E, E_T is the desired threshold energy, σ_o is a scaling factor, and n is an adjustable parameter. The index i denotes vibrational states having energy E_i and population g_i ($\Sigma g_i = 1$), and P_D is the probability that metastable ions formed at particular values of E and E_i will in fact dissociate within the time τ, the average time between excitation in the second quadrupole and mass analysis in the third quadrupole (~ 30 μs). Optimization is carried out by an iterative procedure in which n, σ_o, and E_T are varied to minimize the deviations between the calculated trial function and the experimental appearance curve in the steeply rising portion of the threshold region. The data analysis was performed using the CRUNCH program written by Armentrout and co-workers [13,27]. The region very near and below the threshold is not usually fit because of tailing in the data that is attributed to translational excitation of the ions in the first quadrupole or to internal excitation due to collisions outside the interaction region. This limitation on the fitting range contributes significantly to the relative uncertainty of the derived thresholds.

P_D is determined by performing RRKM calculations of the decay rate as a function of reactant internal energy [13,27–30]. This effect is important because ions with sufficient energy to dissociate may have long enough lifetimes that they fail to decompose within the experimental time window, causing a "kinetic shift" in the apparent threshold [30]. The calculations require several assumptions concerning the reaction. In the present calculations, the experimentally known vibrational frequencies of $CpMn(CO)_3$ [31,32] are used as a model for those of the $CpM(CO)_3^-$ anions. For the $CpM(CO)_2^-$ anions,

Table 1
Vibrational frequency assignments for $CpM(CO)_x^-$ [a]

Frequency (cm^{-1})	Assignment	$x = 3$ CO loss	$x = 2$ CO loss	$x = 1$ CO loss	$x = 1$ Cp^- loss	$x = 0$ Cp^- loss
		Multiplicity				
350	R-M str	1	1	1	1 RC	1 RC
500	M-CO str	1	1	0	0	0
480	M-CO str	2 RC	1 RC	1 RC	1	0
2025	CO str	1	1	0	0	0
1940	CO str	2	1	1	1	0
120	CMC bend	2 T	1 T	0	0	0
100	CMC bend	1	0	0	0	0
140	RMC bend	2 T	2 T	2 TT	2 TT	0
666	MCO bend	1	0	0	0	0
635	MCO bend	2 T	1 T	1 T	1	0
610	MCO bend	1	1	0	0	0
540	MCO bend	2 T	2 T	1 T	1	0
160	RMC twist	1	1	0	0	0
375	R tilt	2	2	2	2 TT	2 TT
3120	CH str	1	1	1	1	1
3098	CH str	2	2	2	2	2
3098	CH str	2	2	2	2	2
1520	CC str	2	2	2	2	2
1428	CC str	2	2	2	2	2
1120	R breathe	1	1	1	1	1
920	R def	2	2	2	2	2
487	R def	2	2	2	2	2
1267	CH def	1	1	1	1	1
1152	CH def	2	2	2	2	2
1056	CH def	2	2	2	2	2
1010	CH def	2	2	2	2	2
848	CH def	1	1	1	1	1
834	CH def	2	2	2	2	2

[a] Frequencies from [32]. Abbreviations used: R = ring, M = metal, str = stretch, def = deformation. The annotations T and TT indicate that one or two of the modes are considered transitional modes; RC indicates the reaction coordinates.

two of the MCO bending frequencies, two of the CMC bending frequencies, one of the M-CO stretching frequencies, and one of the CO stretching frequencies are removed from the $CpM(CO)_3^-$ set. Analogous modifications are made to derive generic frequency sets for $CpMCO^-$ and CpM^-. These frequency sets are summarized in Table 1. The RRKM results and the reactant ion internal energy distribution are not very sensitive to the details of these frequency assignments [11,13]. Most vibrational frequencies of a given type are quite similar in a wide range of cyclopentadienyl metal compounds, as seen for example in the frequencies for Cp_2Fe, $CpMn(CO)_3$, and CpNiNO [31]. Comparison to a partial list of frequencies for $N(CH_3)_4^+[CpCr(CO)_3^-]$ [33] shows no dramatic differences between the frequencies of neutral and anionic cyclopentadienyl metal carbonyl species. Thus, the estimated frequency sets should be sufficiently accurate for the present purposes.

The assignment of vibrational frequencies for the dissociation transition state has a greater effect on the derived threshold. For loss of CO, one of the M-CO stretch frequencies is taken to be the reaction coordinate. Most of the transition state frequencies should be nearly the same as those of the reactant ion. However, two of the MCO bending modes in the reactant become CO rotations in the separated products, and two of the ligand–metal–CO scissor modes become translational degrees of freedom. These "transitional modes" are noted in Table 1. Analogous

assignments for loss of Cp^- are also noted in Table 1. For loss of Co from $CpCo^-$, there are only two transitional modes because no vibrational modes transform into rotational modes when only a single atom is lost.

It is likely that the frequencies for the transitional modes are considerably lower in the transition state than in the excited parent ion. For the present work, as in our previous work on metal carbonyls [11], it is assumed that these four frequencies are reduced by a factor of two in the transition state compared to those in the reactant ion. This corresponds to a vibrational activation entropy of 5.4 eu for CO loss at a nominal temperature of 1000 K [34]. The resulting uncertainty in the threshold analysis is approximated by the difference in the thresholds obtained when the four transitional frequencies are not lowered at all, and when they are all lowered by a factor of four [11], corresponding to a range of vibrational activation entropies from 0–11 eu. The uncertainty is included with the imprecision of the energy scale and the standard deviation of the replicate threshold measurements to derive the final error limits for the bond strengths. The range of activation entropies adopted here includes the values used in RRKM calculations for the dissociation of neutral metal carbonyls [8,35–38] and metal carbonyl cations [13] [29].

Some CID threshold data has been fit with a substantially looser transition state that corresponds to the products at a centrifugal barrier [27]. Such a fitting procedure would raise the reaction thresholds by amounts ranging from 0.09 eV for loss of Cp^- from $CpCo^-$ to 0.44 eV for loss of Cp^- from $CpCoCO^-$. The present fitting procedure is chosen because a moderately loose transition state gives overall activation entropies in better agreement with previous work. For example, loss of CO from $CpM(CO)_3^-$ has a calculated activation entropy of 7.6 eu with a moderately loose transition state and 23.2 eu with a transition state at the centrifugal barrier. Also, the thermochemical cycle discussed below for $CpCo(CO)_n^-$ is less consistent with the bond strengths determined using the loose transition state procedure.

For the data fit in the threshold analyses, the rotational energy content of the reactant is assumed to be conserved on average during the collision with the target gas. Thus, no corrections to the derived thresholds are made for rotational energy effects.

Convoluted into the fit are the reactant ion kinetic energy distribution approximated by a Gaussian function with a 1.5 eV (lab) FWHM and a Doppler broadening function developed by Chantry to account for the random thermal motion of the neutral target [39]. The fits of the steeply rising portion of the data are insensitive to the assigned width of the ion beam energy distribution.

Since internal energy is explicitly taken into account in the threshold analysis, bond energies derived in this manner correspond to 0 K reactants and products. Adjustments to 298 K values [40] can be made using the integrated heat capacities of the reactants and products, with the vibrational energy content of the anions calculated using the estimated vibrational frequencies. To convert to a bond dissociation *enthalpy* term for use in deriving heats of formation, an expansion work factor ΔnRT is also added, where Δn is the change in the number of molecules for the reaction (at 298 K, RT = 2.5 kJ mol^{-1}. The bond enthalpies at 298 K are typically 4 kJ mol^{-1} higher than at 0 K.

3. Results

Collisional activation of the $CpM(CO)_x^-$ in the 0–8 eV (CM) energy range produces fragment ions corresponding to loss of one and two CO molecules, and formation of $C_5H_5^-$. In the $CpCo(CO)_x^-$ systems, up to a few percent of other products are also observed at very high energy. These minor products apparently correspond to ring fragmentation. The fragments produced by CID are similar to those seen previously in the negative ion EI mass spectra of these compounds [15]. The nature of the neutral fragment(s) formed when Cp^- is the ionic product is unknown; the $M(CO)_x$ moiety may depart intact, or the CO ligands and the metal atom may dissociate sequentially. Except for $CpCoCO^-$, loss of one carbonyl ligand is always the dominant process observed in the energy range covered. In this section we first

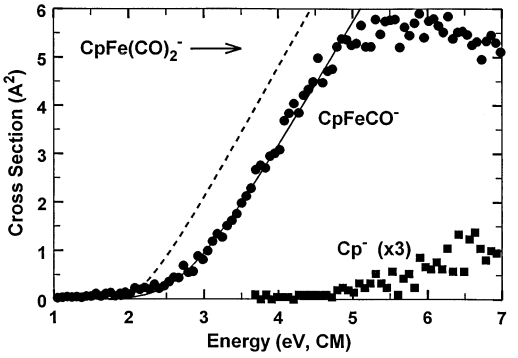

Fig. 1. Appearance curves for products from CID of $CpFe(CO)_2^-$ as a function of kinetic energy. The solid line is a model appearance curve calculated using Eq. (1) and convoluted as discussed in the text, and the dashed line is the unconvoluted fit without internal energy effects or kinetic shifts. The Eq. (1) parameters are E_T = 1.91 eV, n = 1.71.

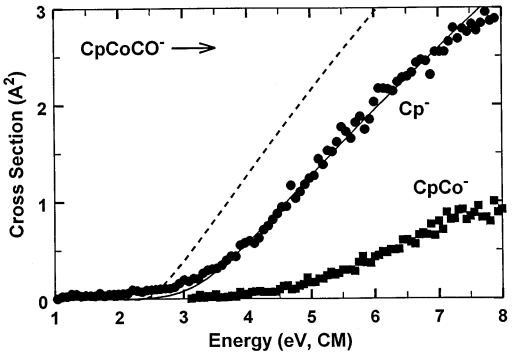

Fig. 3. Appearance curves for products from CID of $CpCoCO^-$ as a function of kinetic energy. The solid line is a model appearance curve calculated using Eq. (1) and convoluted as discussed in the text, and the dashed line is the unconvoluted fit without internal energy effects or kinetic shifts. The Eq. (1) parameters are E_T = 2.38 eV, n = 1.55.

describe the energy-resolved CID behavior of the cyclopentadienyl metal carbonyl anions. The analysis of the CID thresholds is discussed, and metal–carbonyl bond strengths are then derived from these results.

The products observed from CID of the $CpM(CO)_x^-$ ions with argon are given in reactions (2)–(10). The appearance curves for reactions (7)–(9) are shown in Figs. 1, 2, and 3,

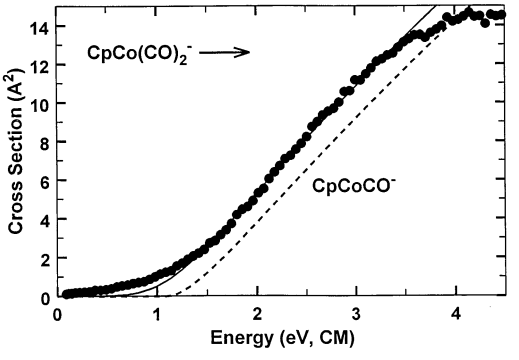

Fig. 2. Appearance curves for products from CID of $CpCo(CO)_2^-$ as a function of kinetic energy. The solid line is a model appearance curve calculated using Eq. (1) and convoluted as discussed in the text, and the dashed line is the unconvoluted fit without internal energy effects or kinetic shifts. The Eq. (1) parameters are E_T = 1.02 eV, n = 1.70.

$$CpV(CO)_3^- \rightarrow CpV(CO)_2^- + CO \quad (2a)$$

$$\rightarrow CpV(CO)^- + 2\,CO \quad (2b)$$

$$\rightarrow Cp^- + [V(CO)_3] \quad (2c)$$

$$CpV(CO)_2^- \rightarrow CpV(CO)^- + CO \quad (3a)$$

$$\rightarrow CpV^- + 2\,CO \quad (3b)$$

$$\rightarrow Cp^- + [VCO_2] \quad (3c)$$

$$CpCr(CO)_3^- \rightarrow CpCr(CO)_2^- + CO \quad (4a)$$

$$\rightarrow CpCr(CO)^- + 2\,CO \quad (4b)$$

$$CpMn(CO)_2^- \rightarrow CpMn(CO)^- + CO \quad (5a)$$

$$\rightarrow CpMn^- + 2\,CO \quad (5b)$$

$$\rightarrow Cp^- + [Mn(CO)_2] \quad (5c)$$

$$CpMn(CO)^- \rightarrow CpMn^- + CO \quad (6a)$$

$$\rightarrow Cp^- + [MnCO] \quad (6b)$$

$$CpFe(CO)_2^- \rightarrow CpFe(CO)^- + CO \quad (7a)$$

$$\rightarrow CpFe^- + 2\,CO \quad (7b)$$

$$\rightarrow Cp^- + [Fe(CO)_2] \quad (7c)$$

Table 2
Optimized fitting parameters for CID reactions[a]

Reactant	Ligand lost	E_T (eV)	n	σ_{max} (Å^2)
$CpV(CO)_3^-$	CO	1.78 ± 0.09	1.6 ± 0.2	16
	2CO			1.4
	Cp^-			0.1
$CpV(CO)_2^-$	CO	1.85 ± 0.13	1.5 ± 0.3	2.5
	2CO			0.1
	Cp^-			0.2
$CpCr(CO)_3^-$	CO	2.03 ± 0.13	1.6 ± 0.2	8
	2CO			0.2
$CpMn(CO)_2^-$	CO	1.81 ± 0.09	1.5 ± 0.2	5
	2CO			3
	Cp^-			1.3
$CpMn(CO)^-$	CO	1.16 ± 0.10	1.6 ± 0.2	5
	Cp^-			5
$CpFe(CO)_2^-$	CO	1.91 ± 0.13	1.5 ± 0.2	6
	2CO			0.1
	Cp^-			0.4
$CpCo(CO)_2^-$	CO	1.02 ± 0.12	1.7 ± 0.2	15
	2CO			0.5
	Cp^-			0.9
$CpCo(CO)^-$	CO			1.0
	Cp^-	2.38 ± 0.14	1.5 ± 0.2	3
$CpCO^-$	Cp^-	1.65 ± 0.13	1.6 ± 0.2	4

[a] Fitting parameters derived using Eq. (1); see text for details.

$$CpCo(CO)_2^- \rightarrow CpCo(CO)^- + CO \quad (8a)$$

$$\rightarrow CpCo^- + 2\,CO \quad (8b)$$

$$\rightarrow Cp^- + [Co(CO)_2] \quad (8c)$$

$$CpCo(CO)^- \rightarrow CpCo^- + CO \quad (9a)$$

$$\rightarrow Cp^- + CoCO \quad (9b)$$

$$CpCo^- \rightarrow Cp^- + CO \quad (10)$$

respectively. The results in Fig. 1 are typical of most of the systems studied, whereas the data in Figs. 2 and 3 show unusually low and high reaction thresholds, respectively. CID threshold plots for the remaining systems are available by request from the corresponding authors.

The maximum cross sections for reactions (2)–(10) in the 0–8 eV energy range are given in Table 2. The maximum total cross sections for all of the reactions examined in this work are in the range of 3–17 Å^2. For comparison, maximum total cross sections for the corresponding $M(CO)_x^-$ ions are 4–28 Å^2 [11].

Table 3
Metal–ligand bond strengths[a]

Bond	0 K	298 K
$Cp(CO)_2V^-$-CO	172 ± 14	176 ± 14
$Cp(CO)V^-$-CO	178 ± 16	182 ± 16
$Cp(CO)_2Cr^-$-CO	196 ± 18	200 ± 18
$Cp(CO)Mn^-$-CO	175 ± 14	179 ± 14
$CpMn^-$-CO	112 ± 11	116 ± 11
$Cp(CO)Fe^-$-CO	184 ± 16	188 ± 16
$Cp(CO)Co^-$-CO	98 ± 12	102 ± 12
$(CO)Co\text{-}Cp^-$	230 ± 19	235 ± 19
$Co\text{-}Cp^-$	159 ± 13	162 ± 13

[a] Bond enthalpies in kJ mol^{-1}.

3.1. CID threshold and bond strength determinations

The optimized fitting parameters obtained with the use of Eq. (1) are listed in Table 2, and three of the corresponding fits are shown in Figs. 1–3. The error limits listed in Table 2 are standard deviations for the parameters optimized for the individual data sets. Optimized fits for the reactions studied have average values of n ranging from 1.5–1.7. Slightly higher values for n (1.6–1.8) were obtained for CID of the metal carbonyl anions [11].

The average vibrational energy of the reactants varies from 10 kJ mol^{-1} for $CpMCO^-$ to 21 kJ mol^{-1} for $CpM(CO)_3^-$. This internal energy lowers the apparent dissociation thresholds. Kinetic shifts raise the apparent thresholds over the actual dissociation thresholds by up to 88 kJ mol^{-1}; the magnitude of the kinetic shift rises rapidly with increasing threshold energy and with increasing size of the reactant ion [41]. Although the two effects work in opposite directions, the effect of kinetic shifts is more important for the larger ions. The reaction thresholds in Table 2 are converted into bond enthalpies at 0 and 298 K in Table 3. The uncertainties in the bond enthalpies in Table 3 also include the uncertainty in the energy scale and the uncertainty arising from modeling the kinetic shifts. The latter uncertainty ranges from 3 kJ mol^{-1} up to 13 kJ mol^{-1} for larger systems with higher thresholds. In some cases, the kinetic shift modeling is the largest contribution to the overall uncertainty.

3.2. Other reaction channels

Threshold measurements for the reaction with the lowest threshold give the most reliable thermochemical results for several reasons. The generally larger cross sections give better signals. Correctly accounting for the energy disposal in multiple ligand dissociations is problematic [29]. Most importantly, lower-energy reactions can substantially affect the measured thresholds for higher-energy reactions because of competitive shifts [42]. Therefore, the thresholds for higher energy reaction channels are not used to derive bond strengths. Qualitatively, however, the secondary thresholds for multiple dissociations are reasonably consistent with the results for two sequential dissociations.

4. Discussion

4.1. Possible sources of systematic experimental error

The first potential difficulty in the analysis of CID thresholds with negative ions is the possibility that electron detachment might compete effectively with dissociation. This could cause a competitive shift in the derived CID thresholds by suppressing the cross sections for CO loss. This possibility has been discussed previously for the case of metal carbonyl anions [10,11], where experimental evidence indicated that electron detachment was not a factor in the threshold analysis even for anions with very low electron binding energies. There is very little information on the electron affinities of the $CpM(CO)_x$ neutrals, but the presence of a Cp ligand, which has an electron affinity of 1.79 eV [43], makes it unlikely that any of the $CpM(CO)_x$ species have low electron affinities. Even the 18-electron complex $CpCo(CO)_2$ has an electron affinity of 0.62 ± 0.10 eV [19] or 0.86 ± 0.2 eV [44]. Therefore, it is assumed that electron detachment does not affect the threshold analysis significantly.

If a dissociation reaction has a reverse activation energy, then the measured dissociation energy will be larger than the actual bond energy. The two plausible causes for a barrier to dissociation are geometric reorganization, and changes in electron configuration between ground state reactants and products. Because the bending potentials in cyclopentadienylmetal carbonyl complexes are generally quite flat, as is evident from their vibrational frequencies, any structural rearrangements accompanying CO dissociation are unlikely to lead to a substantial barrier [45]. Also, for ion dissociations, the relatively long-range ion-induced dipole attraction can dominate minor repulsive interactions along the dissociation pathway [46].

Theoretical considerations indicate that the only component of the change in electron configuration that might lead to a barrier is the spin multiplicity [47]. A reverse activation barrier could occur if the crossing between the potential energy surfaces for the lowest-energy reactant and product spin states were higher in energy than the ground state dissociation products. There are many examples for metal carbonyls where this is known not to be the case, as summarized previously [11].

There is also direct evidence that there is in many cases no reverse activation barrier in cyclopentadienyl metal carbonyl systems. Rapid addition of CO to $CpM(CO)_{x-1}$ indicates that there is no significant barrier to addition, and therefore no barrier in excess of the endothermicity to ligand loss from $CpM(CO)_x$. We observe rapid addition of CO to $CpCo^-$ in the flowing afterglow, although CO does not add to $CpCoCO^-$. Wojcicki and Basolo observed rapid associative exchange of CO ligands for $[CpNiCO]_2$ and $CpCo(CO)_2$ [5]. McLain [48] has noted that CO exchange occurs at room temperature in solutions of $[CpCr(CO)_3]_2$. The exchange was attributed to the 17-electron monomer $CpCr(CO)_3$ that is in equilibrium with the dimer. Zheng et al. have observed moderately fast and temperature-independent addition of CO to CpMnCO and $CpMn(CO)_2$ [49]. CpCoCO, which is apparently a triplet, reacts rapidly with CO in low-temperature matrices [50]. The metal carbonyl cations also do not appear to have barriers associated with conservation of spin during dissociation [13]. Thus, it is probable that there are no significant excess

barriers to the dissociation reactions studied in this article.

However, the need for a spin change may slow down a dissociation reaction, causing an increase in the kinetic shift. Spin-orbit coupling or vibrational coupling of electronic states may be necessary for the electronic state crossing in these systems. The room-temperature addition of CO to triplet $Fe(CO)_4$ to form singlet $Fe(CO)_5$ is slower by a factor of 500 than otherwise similar spin-allowed addition reactions [38]. This reaction, however, involves vibrationally colder reactants because of the room temperature conditions and the absence of any ion-neutral interaction energy. Any kinetic bottlenecks should be smaller in the present experiments because of greater vibrational excitation increasing the coupling of electronic states. Spin changes should be even more efficient in the cyclopentadienyl systems because of the lower symmetry and the larger number of vibrational modes to couple the electronic states. CO adds rapidly to triplet $Cp^*MoCl(PMe_3)_2$ to form a singlet product, although the isolobal addition of N_2 is slow [51]. Therefore, any spin conservation effects in the present systems are presumed to be similar to or smaller than the effect of varying the RRKM parameters discussed above.

4.2. Electronic state effects

The measured thresholds for CO loss from two ions, $CpCo(CO)_2^-$ and $CpMnCO^-$, are substantially below the typical range (175–200 kJ mol^{-1}). The bonding in $CpCo(CO)_2^-$ can be viewed [52] in three ways: as a 19-electron complex with an η^5 Cp ligand, an 18-electron complex with an η^4 Cp ligand, or a 17-electron complex with an η^3 Cp ligand (a slipped ring). These possibilities are sketched in Scheme 1. Which description is most appropriate depends on whether the Cp ligand has all five carbon atoms essentially equidistant from the metal, four carbon atoms closer to the metal (as with a diene ligand), or three carbon atoms closer to the metal (as with an allyl ligand). $CpCo(CO)_3$ has slipped ring [53] and Gregor et al. [15] suggested that $CpCo(CO)_2^-$ has one as well. However, ESR experiments indicate that the η^5 description is most appropriate for $CpCo(CO)_2^-$ [54,55]. Photoelectron spectroscopy studies and ab initio calculations also suggest that the ligand is η^5 [44], although the ring itself is distorted from local fivefold symmetry to twofold symmetry [56]. In this structure, the nineteenth electron must occupy a high-energy orbital. Indeed, the electron affinity of $CpCo(CO)_2$ is comparatively low [19,44]. In any case, all three geometries are consistent with a somewhat weaker Co–CO bond, so the bond strength measurement does not address which structure is correct.

The $CpMnCO^-$ system has a similarly low bond strength. This is most probably because of a mismatch between the preferred electron configurations of $CpMn^-$ and $CpMnCO^-$. Thus, $CpMn^-$ may have to pay a "promotion energy" to reach an excited electronic state more suitable for bonding a CO ligand. This promotion energy could be determined from the energetics of the different electronic states for each species. However, these quantities are unknown experimentally, and accurately calculating the relative energies of different spin states for cyclopentadienyl metal carbonyls is extremely difficult [57–61]. The following discussion should therefore be considered somewhat speculative. First, the 18-electron complexes are taken to be singlets, and the 17- and 19-electron complexes are presumably doublets. The calculations cited above suggest that the lowest singlet and triplet states of 16-electron CpMCO complexes are fairly close in energy, but the most recent work suggests that triplet states are more common [50,61].

Previous work on CpM^- has indicated that "the primary bonding interaction between the metal and

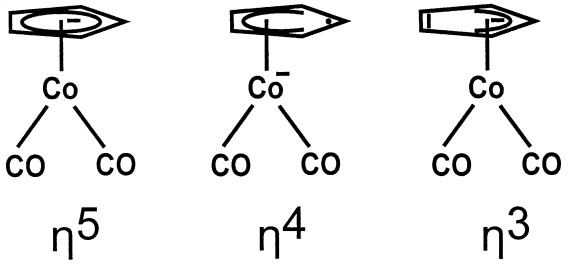

Scheme 1

the ring is a π-type interaction" where electron density is donated from the filled Cp^- HOMO e_1'' orbitals to the d_{xz} and d_{yz} metal orbitals [61]. To form a strong bond, any electrons should be removed from the d_{xz} and d_{yz} orbitals (in the case of s^2d^7 cobalt, one electron must be left in such an orbital). Thus, most of the electronic promotion from the typically high-spin metal atoms to the low-spin 17–19 electron cyclopentadienyl carbonyl complexes presumably occurs with the addition of the Cp^- ligand. Addition of CO ligands should not generally require further promotion, which is consistent with most of the bond energies being nearly equal.

The promotion energy necessary to empty two orbitals is highest for manganese because of the stability of a half-filled 3*d* subshell. Therefore, $CpMn^-$ probably is an exception to the above description with a sextet spin multiplicity and a relatively weak Mn–Cp bond. The low threshold for loss of CO from $CpMnCO^-$, a 15-electron complex that should have either quartet or doublet spin multiplicity, is consistent with the Mn–CO bond energy paying part of the promotion energy cost to reach a lower-spin state that can bind both ligands. $CpMn(CO)_2^-$, which is presumably a 17-electron doublet, does not have a particularly weak Mn–CO bond. This suggests that the promotion energy is small or absent, which would mean that the lowest doublet state of $CpMnCO^-$ is either the ground state or a low-lying excited state.

This promotion energy effect is very similar to that seen for the metal carbonyl anions, where the trends in the M–CO bond strengths suggest that the electronic promotion has usually occurred by the time two CO ligands are bonded to the metal. Again, manganese is the exception; $D[(CO)_2Mn^-–CO]$ is substantially weaker than all other $(CO)_xM^-–CO$ bond strengths for $x \geq 2$ and M = Cr–Co.

Because of insufficient precursor ion intensity, data were not obtained for two other systems, $CpCrCO^-$ and $CpFeCO^-$, where similar effects may occur. However, the small cross sections for loss of 2CO from $CpM(CO)_2^-$ (M = Cr, Fe) suggest that $D(CpM^-–CO)$ is not unusually weak in these systems.

Table 4
Auxiliary thermochemistry[a]

Quantity	Value
$\Delta_fH[CpCo(CO)_{2\ (s)}]$	-169 ± 10
$\Delta_fH(CO)$	-110.5 ± 0.2
$\Delta_fH(C_5H_5^-)$	81 ± 10
$\Delta_fH(Co_{(g)})$	426.8 ± 4.2 [b]
$\Delta_{vap}H[CpMn(CO)_3]$	52 ± 3
$\Delta_{vap}H[CpCo(CO)_2]$	50 ± 10 [c]
EA(Cp)	172 ± 2
$EA[CpCo(CO)_2]$	71 ± 14 [c]

[a] Values (in kJ mol^{-1}) taken from [43] unless otherwise noted.
[b] M.W. Chase, C.A. Davies, J.R. Downey, D.J. Frurip, R.A. McDonald, A.N. Syverud, J. Phys. Chem. Ref. Data 14 (1985) (suppl. 1) (JANAF Tables).
[c] See text.

4.3. $CpCoCO^-$

$CpCoCO^-$ is the only anion studied where loss of Cp^- is apparently lower in energy than loss of CO, as seen in Fig. 3. This is certainly an unexpected result for a 17-electron complex; the other 17-electron complexes, $CpMn(CO)_2^-$ and $CpV(CO)_3^-$, have typical M–CO bond energies. The $COCo–Cp^-$ bond strength is measured to be 230 ± 14 kJ mol^{-1}, so $D(CpCo^-–CO)$ appears to be higher than this value. The data in Fig. 3 show an apparent threshold for loss of CO that is substantially higher than the threshold for loss of Cp^-, but the possibility of a competitive shift means that the apparent threshold may be misleadingly high.

Another approach to the $CpCo^-–CO$ bond enthalpy is to use a thermodynamic cycle to calculate it indirectly. The necessary thermochemistry is given in Table 4. Starting with $\Delta_fH[CpCo(CO)_{2(s)}] = -169 \pm 10$ kJ mol^{-1}, $\Delta_fH[CpCo(CO)_{2(g)}] = -119 \pm 14$ kJ mol^{-1} can be derived using a heat of vaporization estimated from the known value for the similar species $CpMn(CO)_3$. Use of $EA[CpCo(CO)_2] = 71 \pm 14$ kJ mol^{-1}, the average of the two values given above [19,44], then gives $\Delta_fH[CpCo(CO)_{2\ (g)}^-] = -190 \pm 20$ kJ mol^{-1}. The sum of the heats of formation of the fragments, Co + 2CO + Cp^-, is 285 ± 10 kJ mol^{-1}. Thus, the sum of the three stepwise metal–ligand bond dissociation enthalpies is 475 ± 22 kJ mol^{-1}. Subtracting the

bond enthalpies at 298 K for reactions (8a) and (10) gives $D(CpCo^-–CO) = 211 \pm 30$ kJ mol^{-1}. This result is unfortunately subject to six significant accumulated uncertainties, so the final result is very imprecise. The lower limit of 230 ± 14 kJ mol^{-1} derived above suggests that the actual bond enthalpy is around 230 kJ mol^{-1}.

A variation on the above cycle using the same auxiliary thermochemistry and the thresholds for reactions (8a) and (9b) can be used to derive $D(Co\text{-}CO) = 138 \pm 30$ kJ mol^{-1}. This is very similar to the isoelectronic $D(Fe^-–CO) = 141 \pm 15$ kJ mol^{-1} [10].

4.4. Comparisons to $M(CO)_x^-$

In the previous study of metal carbonyl anions [11], 12 M–CO bond strengths ranging from 119–170 kJ mol^{-1} were determined, nine of which were in the range of 150–170 kJ mol^{-1}. Five of the eight M–CO bond strengths measured in the present study are in the range of 172–197 kJ mol^{-1}. This indicates that M–CO bond strengths are increased by the presence of a cyclopentadienyl ligand. The higher bond strengths explain the generally smaller CID cross sections mentioned above.

The cause of this strengthening has been discussed previously [61]. Basically, the Cp ligand and the CO ligands do not interact with the same orbitals on the metal. There is less competition between the ligands for the metal orbitals, and therefore stronger M–CO bonding in the $CpM(CO)_x$ systems. The effect of this competition is evident in the relatively weak $V(CO)_x^-$–CO bonds for $x = 4$ and 5 [11]; an even more extreme case is $Ti(CO)_x^+$ for $x = 5$, 6, and 7 [13].

4.5. Neutral and cationic systems

Unfortunately, it is not possible to derive bond enthalpies for the neutral cyclopentadienylmetal carbonyls from the thermochemical results obtained in this work because of the lack of electron affinity data for the species involved. However, the bond strengths measured here can be compared to the two known neutral CpM–CO bond strengths. Faber and Angelici [62] reported an activation enthalpy of 148 ± 2 kJ mol^{-1} for ligand displacement in solution for the 18-electron species $CpV(CO)_4$; this is somewhat lower than most of the $CpM(CO)_x^-$ bond strengths. In contrast, $D[CpMn(CO)_2–CO]$ is stronger than the anion bond strengths except $D(CpCo^-–CO)$. The cause of the anomalously high bond strengths in $CpMn(CO)_3$ and $CpCoCO^-$ remains unknown.

It has been argued previously that increasing the negative charge on the metal allows stronger ($d\pi$–π^*) back bonding from the metal to the CO ligand [60,63–66]. The present data and the metal carbonyl data both show little difference between the neutral and anion bond energies, but the M–CO bond energies in $M(CO)_x^+$ [13] and $CpM(CO)_x^+$ cations are generally much weaker. Preliminary results from our laboratory give $D(CpMn(CO)_2^+\text{-}CO] = 79 \pm 10$ kJ mol^{-1}, $D[CpMn^+\text{-}CO] = 63 \pm 13$ kJ mol^{-1}, and $D[CpFe^+\text{-}CO] = 50 \pm 11$ kJ mol^{-1}. Appearance potential measurements give $D[CpMn(CO)_2^+–CO] = 63$ kJ mol^{-1} [16] or 30 kJ mol^{-1} [17], and $D[CpV(CO)_2^+\text{-}2CO] = 145$ kJ mol^{-1} [14]. These values are indeed well below the known anion and neutral bond strengths. One apparently stronger cation bond strength is $D[CpCoCO^+\text{-}CO] = 174 \pm 29$ kJ mol^{-1} [14].

4.6. Metal-cyclopentadienide bond energies

Two metal–Cp bond strengths were measured in the course of this study: $D(COCo\text{-}Cp^-) = 230 \pm 14$ kJ mol^{-1} and $D(Co\text{-}Cp^-) = 159 \pm 13$ kJ mol^{-1}. These values are smaller than the average metal–Cp bond energies in metallocenes [67]. However, the CID results in all of the other systems studied indicate that the M–Cp$^-$ bond strengths are higher than the M–CO bond strengths, so the two directly measured values are atypically low. A detailed understanding of the trends in these bond energies must await a more complete set of measurements.

Acknowledgements

This work was supported by the Department of Energy, Office of Basic Energy Science. We thank

Dr. Dingneng Wang for performing preliminary experiments on these systems, and Dr. Leonard Chyall and Dana Byrd for synthesis of $[CpCr(CO)_2]_2$.

References

[1] J.A. Connor, Topics Curr. Chem. 71 (1977) 71.
[2] G. Pilcher, H.A. Skinner, in F.R. Hartley, S. Patai (Eds.), The Chemistry of the Metal–Carbon Bond, Wiley, New York, 1982, Chap. 2.
[3] J.A. Connor, in J.A.M. Simões (Ed.), Energetics of Organometallic Species, NATO ASI Ser. C, Dordrecht, Kluwer, 1992, Vol. 367.
[4] H.A. Skinner, J.A. Conner, in J.F. Liebman, A. Greenburg (Eds.), Molecular Structure and Energetics, VCH, New York, 1987, Vol. 2.
[5] A. Wojcicki, F. Basolo, J. Inorg. Nucl. Chem. 17 (1960) 77.
[6] J.K. Klassen, M. Selke, A.A. Sorensen, G.K. Yang, J. Am. Chem. Soc. 112 (1990) 1267.
[7] T.J. Burkey, J. Am. Chem. Soc. 112 (1990) 8329.
[8] K.E. Lewis, D.M. Golden, G.P. Smith, J. Am. Chem. Soc. 106 (1984) 3905.
[9] J.P. Day, F. Basolo, R.G. Pearson, J. Am. Chem. Soc. 90 (1968) 6927.
[10] L.S. Sunderlin, D. Wang, R.R. Squires, J. Am. Chem. Soc. 114 (1992) 2788.
[11] L.S. Sunderlin, D. Wang, R.R. Squires, J. Am. Chem. Soc. 115 (1993) 12 060.
[12] R.H. Schultz, K.C. Crellin, P.B. Armentrout, J. Am. Chem. Soc. 113 (1991) 8590.
[13] F.A. Khan, D.E. Clemmer, R.H. Schultz, P.B. Armentrout, J. Phys. Chem. 97 (1993) 7978; F. Meyer, Y.-M. Chen, P.B. Armentrout, J. Am. Chem. Soc. 117 (1995) 4071; S. Goebel, C.L. Haynes, F.A. Khan, P.B. Armentrout, ibid., 6994; F.A. Khan, D.L. Steele, P.B. Armentrout, J. Phys. Chem. 99 (1995) 7819; M.R. Sievers, P.B. Armentrout, J. Phys. Chem. 99 (1995) 8135; P.B. Armentrout, Acc. Chem. Res. 28 (1995) 430; F. Meyer, P.B. Armentrout, Mol. Phys. 88 (1996) 187.
[14] R.E. Winters, R.W. Kiser, J. Organomet. Chem. 4 (1965) 190.
[15] M.R. Blake, J.L. Garnett, I.K. Gregor, S.B. Wild, Org. Mass Spectrom. 13 (1978) 20.
[16] J. Müller, M. Herberhold, J. Organomet. Chem. 13 (1968) 399.
[17] A. Efraty, M.H.A. Huang, C.A. Weston, Inorg. Chem. 11 (1975) 2796.
[18] R.R. Corderman, J.L. Beauchamp, Inorg. Chem. 16 (1977) 3135.
[19] R.N. McDonald, P.L. Schell, Organometallics 7 (1988) 1806.
[20] K.J. van den Berg, S. Ingemann, N.M.M. Nibbering, Organometallics 11 (1992) 2389.
[21] I.K. Gregor, M. Guilhaus, Mass Spectrom. Rev. 3 (1984) 39.
[22] R.R. Squires, Chem. Rev. 87 (1987) 623.
[23] S.T. Graul, R.R. Squires, Mass Spectrom. Rev. 7 (1988) 263.
[24] P.J. Marinelli, J.A. Paulino, L.S. Sunderlin, P.G. Wenthold, J.C. Poutsma, R.R. Squires, Int. J. Mass Spectrom. Ion Processes 130 (1994) 89.
[25] P.H. Dawson (Ed.), Quadrupole Mass Spectrometry and its Applications, Elsevier, New York, 1976; P.E. Miller, M. Bonner Denton, Int. J. Mass Spectrom. Ion Processes 72 (1986) 223.
[26] R. Birdwhistell, P. Hackett, A.R. Manning, J. Organomet. Chem. 157 (1978) 239.
[27] S.K. Loh, D.A. Hales, L. Lian, P.B. Armentrout, J. Chem. Phys. 90 (1989) 5466; L. Lian, C.-X Su, P.B. Armentrout, J. Chem. Phys. 96 (1992) 7542; M.T. Rodgers, K.M. Ervin, P.B. Armentrout, J. Chem. Phys. 106 (1997) 4499.
[28] W. Yu, X. Liang, R.B. Freas, J. Phys. Chem. 95 (1991) 3600.
[29] D.V. Dearden, K. Hayashibara, J.L. Beauchamp, N.J. Kirchner, P.A.M. van Koppen, M.T. Bowers, J. Am. Chem. Soc. 111 (1989) 2401.
[30] J.P. Robinson, K.A. Holbrook, Unimolecular Reactions, Wiley-Interscience, New York, 1972; W. Forst, Theory of Unimolecular Reactions, Academic, New York, 1973.
[31] I.J. Hyams, R.T. Bailey, E.R. Lippincott, Spectrochim. Acta A 23 (1967) 273.
[32] D.M. Adams, A. Squire, J. Organomet. Chem. 63 (1973) 381; K. Chhor, G. Lucazeau, Inorg. Chem. 23 (1984) 462.
[33] V.R. Feld, E. Hellner, A. Klopsch, K. Dehnicke, Z. Anorg. Allg. Chem. 442 (1978) 173.
[34] T. Baer, J. Boze, K.-M. Weizel, in C.Y. Ng (Ed.), Vacuum UV Photoionization and Photodissociation of Molecules and Clusters, World Scientific, Singapore, 1991.
[35] T.R. Fletcher, R.N. Rosenfeld, J. Am. Chem. Soc. 107 (1985) 2203; 110 (1988) 2097.
[36] D.M. Rayner, Y. Ishikawa, C.E. Brown, P.A. Hackett, J. Chem. Phys. 94 (1991) 5471.
[37] B. Venkataraman, H. Hou, Z. Zhang, S. Chen, G. Bandukwalla, M. Vernon, J. Chem. Phys. 92 (1990) 5338.
[38] E. Weitz, J. Phys. Chem. 91 (1987) 3945.
[39] P.J. Chantry, J. Chem. Phys. 55 (1971) 2746.
[40] S.G. Lias, J.E. Bartmess, J.F. Liebman, J.L. Holmes, R.D. Levin, W.G. Mallard, J. Phys. Chem. Ref. Data 17 (1988) (suppl. 1).
[41] R.G. Cooks, J.H. Beynon, R.M. Caprioli, G.R. Lester, Metastable Ions, Elsevier, Amsterdam, 1973.
[42] C. Lifshitz, F.A. Long, J. Chem. Phys. 41 (1964) 2468.
[43] W.G. Mallard, P.J. Linstrom (Eds.), NIST Chemistry WebBook, NIST Standard Reference Database Number 69, March 1998, National Institute of Standards and Technology, Gaithersburg, MD (http://webbook.nist.gov).
[44] J.M. Campbell, A.A. Martel, S.-P. Chen, I.M. Waller, J. Am. Chem. Soc. 119 (1997) 4678.
[45] C.D. Hoff, Prog. Inorg. Chem. 40 (1992) 503.
[46] V.L. Talrose, P.S. Vinogradov, I.K. Larin, in M.T. Bowers (Ed.), Gas Phase Ion Chemistry, Academic Press, New York, 1979, Vol. 1.
[47] P.B. Armentrout, J. Simons, J. Am. Chem. Soc. 114 (1992) 8627.
[48] S.L. McLain, J. Am. Chem. Soc. 110 (1988) 643.
[49] Y. Zheng, W. Wang, J. Lin, Y. She, K. Fu, J. Phys. Chem. 96 (1992) 7650.
[50] A.A. Bengali, R.G. Bergman, C.B. Moore, J. Am. Chem. Soc. 117 (1995) 3879.

[51] D.W. Keogh, R. Poli, J. Am. Chem. Soc. 119 (1997) 2516.
[52] R.M. Kowaleski, F. Basolo, W.C. Trogler, R.W. Gedridge, T.D. Newbound, R.D. Ernst, J. Am. Chem. Soc. 109 (1987) 4860.
[53] O. Crichton, A.J. Rest, D.J. Taylor, J. Chem. Soc. Dalton Trans. (1980) 167.
[54] N.G. Connelly, W.E. Geiger, G.A. Lane, S.J. Raven, P.H. Rieger, J. Am. Chem. Soc. 108 (1986) 6219; W.E. Geiger, Acc. Chem. Res. 28 (1995) 351.
[55] D.A. Braden, D.R. Tyler, J. Am. Chem. Soc. 120 (1998) 942.
[56] L.R. Byers, L.F. Dahl, Inorg. Chem. 19 (1980) 277.
[57] M. Elian, M.M.L. Chen, M.P. Mingos, R. Hoffmann, Inorg. Chem. 15 (1976) 1148; T.A. Albright, R. Hoffmann, Chem. Ber. 111 (1978) 1578.
[58] P. Hofmann, Angew. Chem. Int. Ed. Engl. 16 (1977) 536; P. Hofmann, M. Padmanabhan, Organometallics 2 (1983) 1273.
[59] D.L. Lichtenberger, R.F. Fenske, J. Am. Chem. Soc. 98 (1976) 50.
[60] T. Ziegler, V. Tschinke, L. Fan, A.D. Becke, J. Am. Chem. Soc. 111 (1989) 9177.
[61] P.E.M. Siegbahn, J. Am. Chem. Soc. 118 (1996) 1487.
[62] G.C. Faber, R.J. Angelici, Inorg. Chem. 9 (1970) 1587; ibid., 23 (1984) 4781.
[63] C.W. Bauschlicher, P.S. Bagus, C.J. Nelin, B.O. Roos, J. Chem. Phys. 85 (1986) 354.
[64] K.G. Caulton, R.F. Fenske, Inorg. Chem. 7 (1968) 1273; K. Pierloot, J. Verhulst, L.G. Vanquickenborne, Inorg. Chem. 28 (1989) 3059.
[65] N.A. Beach, H.B. Gray, J. Am. Chem. Soc. 90 (1968) 5713.
[66] J. Koutecky, G. Pacchioni, P. Fantucci, Chem. Phys. 99 (1985) 87.
[67] D.E. Richardson, in J.A.M. Simões (Ed.), Energetics of Organometallic Species, NATO ASI Series C, Dordrecht, Kluwer, 1992, Vol. 367.